Stereospecificity of fatty acid 2-hydroxylase and differential functions of 2-hydroxy fatty acid enantiomers[S]

Lin Guo,* Xu Zhang,* Dequan Zhou,* Adewole L. Okunade,* and Xiong Su[1],*,[†]

Department of Internal Medicine, Center for Human Nutrition,* and Department of Cell Biology and Physiology,[†] Washington University School of Medicine, St. Louis, MO 63110

Abstract FA 2-hydroxylase (FA2H) is an NAD(P)H-dependent enzyme that initiates FA α oxidation and is also responsible for the biosynthesis of 2-hydroxy FA (2-OH FA)-containing sphingolipids in mammalian cells. The 2-OH FA is chiral due to the asymmetric carbon bearing the hydroxyl group. Our current study performed stereochemistry investigation and showed that FA2H is stereospecific for the production of (R)-enantiomers. FA2H knockdown in adipocytes increases diffusional mobility of raft-associated lipids, leading to reduced GLUT4 protein level, glucose uptake, and lipogenesis. The effects caused by FA2H knockdown were reversed by treatment with exogenous (R)-2-hydroxy palmitic acid, but not with the (S)-enantiomer. Further analysis of sphingolipids demonstrated that the (R)-enantiomer is enriched in hexosylceramide whereas the (S)-enantiomer is preferentially incorporated into ceramide, suggesting that the observed differential effects are in part due to synthesis of sphingolipids containing different 2-OH FA enantiomers.[jlr] These results may help clarify the mechanisms underlying the recently identified diseases associated with FA2H mutations in humans and may lead to potential pharmaceutical and dietary treatments. This study also provides critical information to help study functions of 2-OH FA enantiomers in FA α oxidation and possibly other sphingolipid-independent pathways.—Guo, L., X. Zhang, D. Zhou, A. L. Okunade, and X. Su. **Stereospecificity of fatty acid 2-hydroxylase and differential functions of 2-hydroxy fatty acid enantiomers.** *J. Lipid Res.* 2012. 53: 1327–1335.

Supplementary key words 2-hydroxy fatty acid • FA 2-hydroxylase • chirality • membrane fluidity • glucose transporter 4 • glucose uptake • adipocyte

FA hydroxylation alters the packing structures of membrane microdomains and thus could regulate cellular functions of membrane-associated proteins (1). FA 2-hydroxylase (FA2H) is a recently identified NAD(P)H-dependent enzyme that catalyzes the hydroxylation of FA at the C-2 position to produce 2-hydroxy FAs (2-OH FAs) (**Scheme 1**) (2, 3). In addition to undergoing α oxidation to form odd-chain-length FAs (4), the FA2H-generated 2-OH FAs are incorporated into a long-chain sphingosine base via an amide bond to generate 2-hydroxy sphingolipids (2-OH sphingolipids) (Scheme 1) (5). The 2-OH sphingolipids are important components of plasma membrane lipid rafts, which host a variety of signaling and trafficking events. Specific functions of 2-OH sphingolipids in membrane endocytosis were first demonstrated in *Saccharomyces cerevisiae* yeast strains with defective SCS7/FA2H (6, 7). Recent genetic studies suggest a critical role of FA2H and possibly 2-OH sphingolipids in multiple neurodegenerative diseases. Loss of FA2H in mice causes significant demyelination and profound axonal loss (8, 9). Mutations in the FA2H gene in humans are associated with leukodystrophy (10), spastic paraplegia (11), and neurodegeneration with brain iron accumulation (12). FA2H may also play a significant role in metabolism. We recently showed decreased levels of glucose transporter 4 (GLUT4) proteins and thus cellular glucose uptake in FA2H knockdown adipocytes (13). A recent study also suggested a role of FA2H in synthesis of specific sebaceous gland or sebum lipids and in regulating the hair follicle homeostasis (14).

2-OH FAs are chiral due to the asymmetric carbon bearing the hydroxyl group, and a specific 2-hydroxylase usually generates enantiopure products. Biological samples and diets therefore have different enantio-enrichments of

Abbreviations: Cer, ceramide; CHO, Chinese hamster ovary; CTxB, cholera toxin subunit B; D, diffusion coefficient; FA2H, FA 2-hydroxylase; FAME, FA methyl ester; FRAP, fluorescence recovery after photobleaching; GLUT4, glucose transporter 4; HexCer, hexosylceramide; Mf, mobile fraction; MTPA, α-methoxy-α-trifluoromethylphenylacetyl; NCI-MS, negative chemical ionization mass spectrometry; NL, neutral loss; 2-OH Cer, 2-hydroxy ceramide; 2-OH FA, 2-hydroxy FA; 2-OH PA, 2-OH palmitic acid; 2-OH sphingolipid, 2-hydroxy sphingolipid; ROI, region of interest; PA, palmitic acid; (R)-MTPA-Cl, (R)-MTPA chloride; SCD1, stearoyl-CoA desaturase 1; siRNA, small interfering RNA.

[1]To whom correspondence should be addressed.
 e-mail: xsu@wustl.edu
[S] The online version of this article (available at http://www.jlr.org) contains supplementary data in the form of six figures.

Scheme. 1. Metabolic fates of FA2H-generated 2-OH FA.

2-OH FAs. Wool wax 2-OH FAs are found exclusively in the (*R*) form, whereas in bacterial lipopolysaccharides, (*S*)-2-OH FAs are the major form (15, 16). Most food and animal tissue samples, including fat (suet) (17), have both enantiomers (16). However, there is lack of information on which enantiomer is generated by FA2H and on whether both enantiomers are biologically active. Moreover, due to the lack of stereochemistry information on FA2H, racemic 2-OH FAs, but not 2-OH FA enantiomers were used to explore its potential role or to reverse effects of FA2H deficiency (7, 13). In the current study, we examined the stereospecificity of FA 2-hydroxylation catalyzed by FA2H. We further investigated the specific biological functions of the 2-OH FA enantiomers and their incorporation into sphingolipids.

EXPERIMENTAL PROCEDURES

Materials

FBS, calf serum, DMEM, Silencer™ small interfering RNA (siRNA) construction kit, Lipofectamine™ RNAiMAX, and Alex 488-labeled cholera toxin subunit B (CTxB) were ordered from Invitrogen. Rabbit anti-GLUT4 antibody was kindly provided by Dr. Michael Mueckler (Washington University, St. Louis, MO). Rabbit anti-FA2H antibody was kindly provided by Dr. Hiroko Hama (Medical University of South Carolina, Charleston, SC). 2-OH palmitic acid (2-OH PA) was obtained from TCI America. Other reagents were from Sigma.

Culture and treatment of 3T3-L1 adipocytes

3T3-L1 adipocytes were cultured and differentiated as described (13). Adipocytes were used 6–8 days after initiation of differentiation. Mouse FA2H siRNA synthesis and transfection were performed exactly as described (13). Twenty-four hours post transfection, cells were switched to growing media with 50 μM 2-OH PA enantiomers. Two days later, fluorescence recovery after photobleaching (FRAP) experiment, glucose uptake assay, lipogenesis, quantitative RT-PCR, or Western blotting were performed as we previously described (13).

Generation of Chinese hamster ovary cell line stably over-expressing FLAG-hFA2H

Chinese hamster ovary (CHO) cells were cotransfected with pcDNA3-FLAG-hFA2H (2) and pTK-hyg vector (Clontech) at a 20:1 ratio using lipofectamine 2000 as previously described (18). The cells were then selected with 150 μg/ml hygromycin (Invitrogen). After 3 weeks, hygromycin-resistant colonies started to grow. Individual colonies were isolated using cloning cylinders

(Sigma) and transferred to 24-well plates in duplicate. Recombinant FA2H proteins containing the FLAG epitope in one well were verified by Western blot analysis with anti-FA2H or anti-FLAG antibody (Cell Signaling Technology), and clones with protein expression were selected and diluted in media with 150 μg/ml hygromycin. Around 2 weeks later, hygromycin-resistant colonies were isolated again and clones with protein expression were selected and scaled up for further assays.

Lipid extraction and derivatization of 2-hydroxy FAs (2-OH FAs)

Cells cultured in 10 cm plates were washed with PBS and scraped into PBS. Cell pellets were collected by centrifugation in 10 ml glass tubes with screw caps. FA methyl esters (FAMEs) were prepared by reaction with methanol-acetyl chloride (2:1, v/v) at 70°C as described (19). Hydroxy FAMEs were then separated on silica gel 60A plates (Whatman; Clifton, NJ) using a mobile phase of hexane-diethyl ether-acetic acid (70:30:1, v/v/v). Spots corresponding to 2-hydroxy FAMEs were visualized with 0.01% rhodamine 6G and identified with standards. The bands were scraped and extracted with chloroform-methanol (3:1, v/v) and further derivatized with (*R*)-α-methoxy-α-trifluoromethylphenylacetyl (MTPA) chloride ((*R*)-MTPA-Cl) (15) prior to gas chromatography negative chemical ionization mass spectrometry (GC-NCI-MS) analysis.

Enantiopurification of 2-OH PA

Purification of 2-OH PA enantiomers was achieved by recrystallization from commercially available racemic 2-OH PA as described (20). Briefly, 1 g racemic acid dissolved in 50 ml of ether was added to a solution of 0.425 g (*S*)-(−)-α-methybenzylamine (Sigma) or (*R*)-(+)-α-methybenzylamine (Sigma) in 100 ml of light petroleum (boiling point 50–70°C), respectively. After crystallization three times from light petroleum-ether (2:1, v/v), the resulting diastereomeric salts of 2-OH PA were acidified with 10% HCl and extracted with ether. The ether layers were washed until neutral and dried to give respective 2-OH PA enantiomers. The absolute configurations of purified 2-OH PA enantiomers were determined by GC-NCI-MS analysis after methylation of the carboxyl group and subsequent esterification of the hydroxyl group with Mosher's reagent.

GC-NCI-MS analysis of MTPA derivatives of 2-OH PA methyl ester

GC-MS analyses were performed with Hewlett-Packard 6890 series gas chromatograph interfaced to an Agilent 5973N mass spectrometer in negative chemical ionization mode. Samples were separated on a DB-5MS column (30 m × 0.25 mm × 0.25 m; Agilent). Ultra-high-purity helium was used as the carrier gas at a constant flow rate of 1.0 ml/min and methane as the reagent gas with a flow rate of 2.0 ml/min. The column temperature was initially held at 100°C and then raised to 280°C at a rate of 30°C/min, followed by an isothermal period of 5 min. The total run time was 11.0 min. The injector and transfer line temperatures were set at 250°C and 280°C, respectively. One microliter of sample in heptane was injected with a 7683 autosampler on split mode with a split ratio of 1:5. A solvent delay of 4 min was applied. The MS ion source temperature was kept at 200°C. The MS was run in the full scan mode at 2.69 cycles/second, with electron energy of 70 eV.

Lipid extraction and analysis of sphingolipids by ESI MS

Adipocytes cultured in 10 cm plates were washed with PBS, collected, and resuspended in 0.5 ml PBS. After spiking 500 pmol of each component of ceramide/sphingoid internal standards mixture I (Avanti Polar Lipids, LM-6002), lipids were extracted as

described (21) and reconstituted in 100 μl of methanol for sphingolipid analysis. Individual ceramide (Cer) and 2-hydroxy ceramide (2-OH Cer) molecular species were examined by ESI-MS/MS in the negative-ion mode as [M-H]⁻ on a Finnigan TSQ Vantage mass spectrometer by direct infusion of the sample into the ESI chamber as described (22). Cer and 2-OH Cer molecular species were fingerprinted by the neutral loss (NL) scanning of fragments of m/z 256 and 327, respectively. Individual SM molecular species were identified by ESI-MS/MS with the NL scanning of m/z 213 in the positive-ion mode as [M+Li]⁺ as described (23).

Quantitative analysis of 2-OH Cer and 2-OH hexosylceramide (2-OH HexCer) was performed as described (21) by LC ESI-MS/MS on an Agilent 1100 LC system connected to an Agilent 6460 triple quadrupole mass spectrometer. A Phenomenex Lunar Silica (2) column (150 × 2 mm i.d., 5 μm particle size) was used. The mobile phases consisted of acetonitrile-methanol-acetic acid (97:2:1, v/v/v) (A) and methanol-acetic acid (99:1, v/v) (B) containing 5 mM ammonium acetate. The gradient elution was programmed as follows: 0–3 min 100% A; 3–4 min 100–0% A; 4–5 min 0% A; 5–6 min 0–100% A. The mobile-phase flow rate was maintained at 0.2 ml/min, and the column temperature was kept at 30°C. The injection volume was 10 μl.

Statistical analyses

The data are presented as means ± SE. The results were analyzed by one-way ANOVA followed by post hoc t-test. A P value < 0.05 was considered statistically significant.

RESULTS

Stereospecific generation of (R)-2-OH FA by FA2H

We prepared the optically pure 2-hydroxy palmitic acids, (R)-2-hydroxy palmitic acid [(R)-2-OH PA] and (S)-2-hydroxy palmitic acid [(S)-2-OH PA], by multiple recrystallization using commercially available racemic 2-OH PAs. To determine their absolute configurations, the resulting (R)- and (S)-2-OH PA were converted to the corresponding (R)-Mosher esters by methylation of the carboxyl group and subsequent esterification of the hydroxyl group with Mosher's reagent, (R)-MTPA-Cl. As illustrated in **Fig. 1**, the diastereomeric MTPA derivatives of (R)- and (S)-2-OH PA were well separated by GC and identified by NCI-MS (Fig. 1C, D). By comparison with the retention times and fragmentation patterns in the mass spectra of (R)-MTPA derivatives of racemic 2-OH PA (Fig. 1A) and wool wax that contains enantiopure (R)-2-OH PA (Fig. 1B), the peak eluted at 8.40 min is attributed to (S)-2-OH PA (Fig. 1D), whereas the latter at 8.56 min is assigned to (R)-enantiomer (Fig. 1C). The MTPA derivatives of both enantiomers gave a strong characteristic fragment ion at m/z 471, [M-31]⁻. This ion results from the elimination of a methoxy group attached to the MTPA moiety after α-cleavage (15). The fragment ions at m/z 269 and m/z 189 represent the methyl palmitate and the MTPA moieties, respectively (**Fig. 2**) (15).

To check the stereospecificity of FA2H, we stably overexpressed human FA2H (hFA2H) with a FLAG tag in CHO cells, where endogenous FA2H activity is low. Western blot analysis verified the overexpression of hFA2H in this cell line (Fig. 1G). Cellular lipids were extracted,
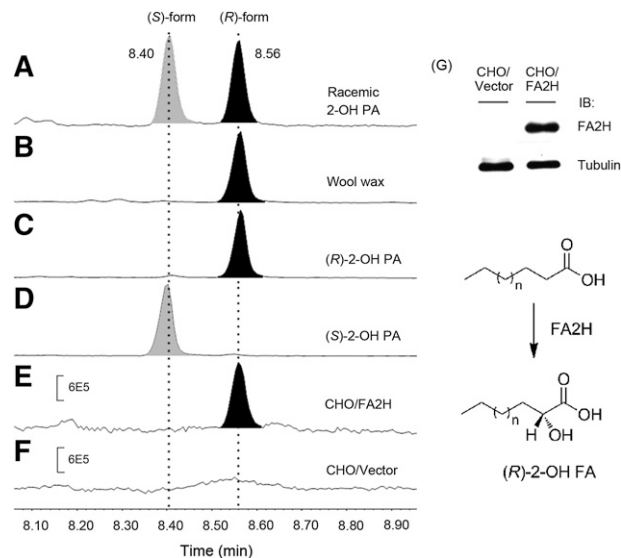

Fig. 1. Generation of (R)-2-OH FA by FA2H. GC-NCI-MS analysis of the absolute configuration of 2-OH PA in racemic 2-OH PA (A), wool wax containing enantiopure (R)-2-OH PA (B), purified (R)-2-OH PA (C), and (S)-2-OH PA (D), CHO cells overexpressing hFA2H (E), and control CHO cells with vector (F). The enzyme expression in CHO cells was evaluated by immunoblotting (IB) using antibody recognizing hFA2H (G). In conclusion, FA2H is stereospecific for the production of the (R)-enantiomer of 2-hydroxy FAs.

and 2-OH FAMEs were prepared by methylation prior to separation on a silica plate. The isolated 2-OH FAMEs were then derivatized with (R)-MTPA-Cl and analyzed by GC-NCI-MS. As shown in Fig. 1, neither (R)-2-OH PA nor (S)-2-OH PA was detected in the control CHO cells due to low FA2H activity (Fig. 1F). Overexpression of hFA2H in CHO cells exclusively produces (R)-2-OH PA, but not (S)-2-OH PA, as only one chromatographic peak was recorded at 8.56 min (Fig. 1E), which is identical to those of authentic (R)-2-OH PA from wool wax (Fig. 1B) and purified standard (Fig. 1C). NCI-MS spectrum of the peak gives fragment ions at m/z 471, 269, and 189, which are identical to those from purified standard. These results
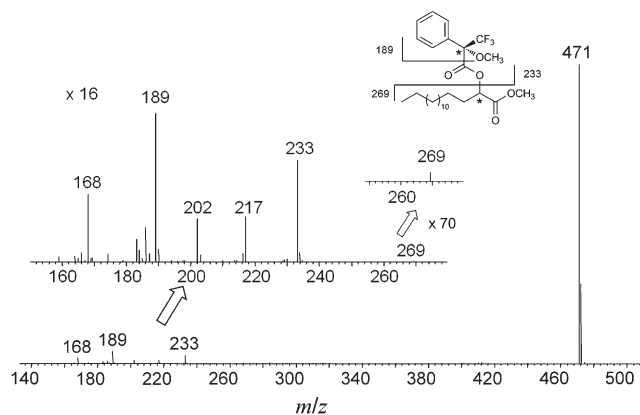

Fig. 2. NCI mass spectrum of MTPA derivative of 2-OH PA methyl ester.

confirmed the stereospecificity of FA2H for the production of (*R*)-enantiomeric 2-OH FAs.

(*R*)-2-OH PA, but not (*S*)-2-OH PA reverses enhanced membrane mobility by FA2H silencing in adipocytes

2-OH sphingolipids are important constituents of lipid rafts at the cellular membrane. We previously demonstrated that FA2H knockdown in adipocytes by RNA interference enhanced raft fluidity by FRAP experiment, and racemic 2-OH PA partially reversed this effect (13). Because FA2H is stereospecific for the production of the (*R*) form of 2-OH PA, we compared the differential effects of 2-OH PA enantiomers to reverse the enhanced raft fluidity in FA2H knockdown adipocytes. Accordingly, we used Alexa-488 conjugated CTxB to label the lipid rafts of the FA2H knockdown adipocytes that were preincubated with (*R*)-2-OH PA and (*S*)-2-OH PA, respectively. After photobleaching a region of interest (ROI) on the rim of fluorescent CTxB-labeled plasma membrane with high intensity laser, fluorescence recovery in the bleached ROI was recorded and quantified by calculating the mobile fraction (Mf) and diffusion coefficient (D) as described previously (13). Mf and D represent the degree and rate of diffusive exchange of bleached CTxB molecules with adjacent unbleached fluorescent CTxB molecules, and thus are positively related to the fluidity of CTxB-labeled lipid rafts. The fluorescence recovery of individual experiments is shown in supplementary Fig. I. The representative images are presented in **Fig. 3A** and supplementary Fig. II. As shown in Fig. 3, over the time course of the experiments, after treatment with (*R*)-2-OH PA in FA2H-depleted adipocytes, Mf was decreased from 27 ± 2.5 to $11 \pm 1.3\%$ and D from 0.24 ± 0.02 to 0.10 ± 0.01 $\mu m^2 s^{-1}$, in close proximity to those in control adipocytes, confirming that the (*R*) form of 2-OH PA reversed the increased raft fluidity induced by FA2H knockdown. In contrast, treatment with (*S*)-2-OH PA gave rise to a further enhancement of the raft fluidity, with Mf and D increased up to $37 \pm 2.6\%$ and 0.29 ± 0.03 $\mu m^2 s^{-1}$, respectively.
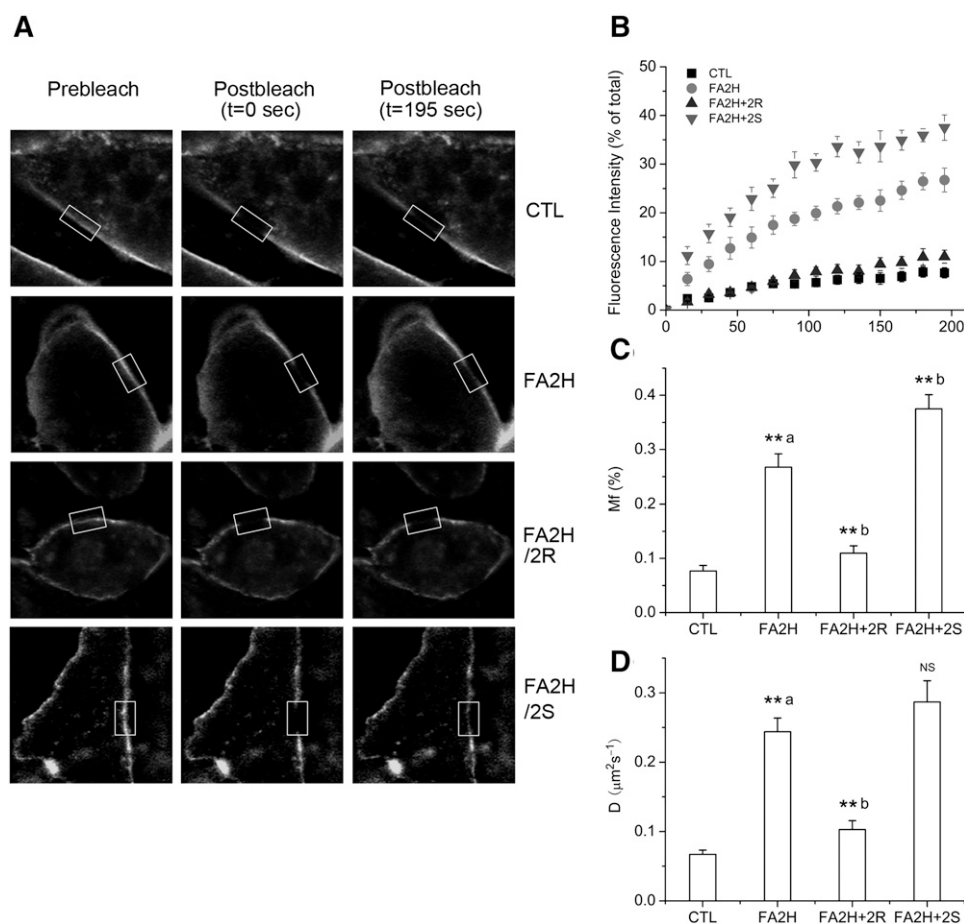

Fig. 3. Stereospecific rescuing effect of 2-OH PA on accelerated raft fluidity induced by FA2H depletion. 3T3-L1 adipocytes were treated with a negative control siRNA (CTL) or an siRNA recognizing FA2H (FA2H). Twenty-four hours post transfection, 50 µM (*R*)-2-OH PA (2R) or (*S*)-2-OH PA (2S) was added as indicated. Labeling with Alex 488-CTxB and FRAP measurements were performed. A: Selected images from a confocal FRAP experiment in adipocytes labeled with Alexa 488-CTxB at room temperature. B: Kinetics of recovery for Alexa 488-CTxB. Each curve represents means ± SE from 10 experiments. The fluorescence recovery of individual experiments is shown in supplementary Fig. I. C: Calculated Mfs. D: Diffusion coefficients (D). **[a] $P < 0.01$ (compared with CTL). **[b] $P < 0.01$ (compared with FA2H). NS, nonsignificant (compared with FA2H).

Regulation of GLUT4 level, glucose uptake, and lipogenesis by 2-OH PA enantiomers in FA2H knockdown adipocytes

We further studied some of the biological consequences of the regulated raft fluidity by FA2H and 2-OH FA enantiomers. GLUT4 is the major insulin-responsive glucose transporter in muscle and adipose, and its activity on glucose uptake is determined by protein level and plasma membrane localization. Lipid rafts play important roles in determining GLUT4 trafficking, degradation, and glucose uptake (24, 25). Knockdown of FA2H in adipocytes decreases the protein level of GLUT4 and thus impairs glucose uptake under basal and insulin-stimulated conditions, due to the accelerated raft fluidity that promotes degradation of GLUT4 (13). Because the increased raft fluidity can only be reversed by the (R) form of 2-OH PA, we asked whether (R)-2-OH PA is also specific to reverse the effects of FA2H knockdown on GLUT4 level and function. We measured protein levels of GLUT4 and glucose uptake after treatment with (R)-2-OH PA or (S)-2-OH PA in FA2H knockdown adipocytes. Because FAS and stearoyl-CoA desaturase 1 (SCD1) levels are correlated with glucose utilization (26), we also measured FAS and SCD1 mRNA levels. As shown in **Fig. 4**, in FA2H-depleted adipocytes, the decreased GLUT4 levels (Fig. 4A, B), rates of glucose uptake (Fig. 4C), FAS and SCD1 mRNA levels (Fig. 4D, E), and lipogenesis (Fig. 4F) were reversed by treatment with (R)-2-OH PA. In contrast, a further reduction or no effect was observed for (S)-2-OH PA (Fig. 4). Levels of caveolin-1 proteins were not changed, either by FA2H knockdown or

treatment with 2-OH PA enantiomers (Fig. 4A), suggesting that FA2H and caveolin-1 are independent determinants of raft mobility and GLUT4 levels. The levels of preadipocyte factor-1 (pref-1) are not changed either (see supplementary Fig. III), and together with unchanged levels of caveolin-1 (Fig. 4A) and adipocyte FA binding protein (AP2) (13), argue against adipocyte dedifferentiation by FA2H knockdown. These results, together with the specific effects of (R)-2-OH PA on raft fluidity, provided further support for the stereospecificy of FA2H for the production of the (R) form of 2-OH FA and suggested that (R)-2-OH PA is more potent and appropriate than racemic 2-OH PA to reverse effects caused by FA2H deficiency.

Regulation of 2-OH sphingolipids in adipocytes by FA2H knockdown and 2-OH PA enantiomers

To confirm whether FA2H regulates raft mobility and GLUT4 levels via synthesis of 2-OH sphingolipids, we first identified 2-OH sphingolipids in 3T3-L1 adipocytes. Negative-ion ESI-MS/MS spectroscopic analyses (NL of a fragment at m/z 256) of total lipid extracts demonstrated significant amounts of Cers in adipocytes with the most-abundant peaks at m/z 536 (C16:0 Cer) and 662 (C25:0 Cer or C24:1 2-OH Cer) (**Fig. 5A**). A peak at m/z 552 suggested the presence of C16:0 2-OH Cer (Fig. 5A, insert). Because 2-OH Cer is much less sensitive than nonhydroxy Cer in the NL of m/z 256 (22), we further fingerprinted 2-OH Cer species by performing NL scanning of a fragment at m/z 327, characteristic of 2-OH Cer species (22). As shown in Fig. 5B, C16:0 2-OH Cer at m/z 552 is the
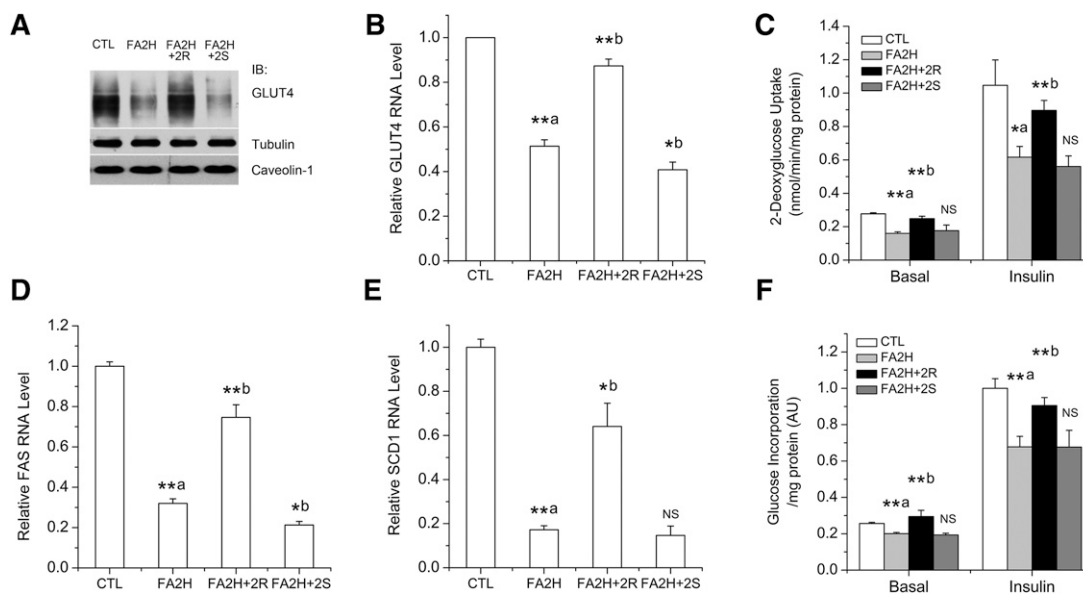

Fig. 4. Differential roles of 2-OH PA enantiomers on GLUT4 levels and activities in FA2H knockdown adipocytes. 3T3-L1 adipocytes were treated with a negative control siRNA (CTL) or an siRNA recognizing FA2H (FA2H). Twenty-four hours post transfection, 50 μM (R)-2-OH PA (2R) or (S)-2-OH PA (2S) was added as indicated. A: Whole-cell lysates were prepared and analyzed by immunoblotting using antibodies recognizing GLUT4, tubulin, and caveolin-1. B: Band intensities of GLUT4 were quantified from four independent experiments with ImageJ software. The data represent the means ± SE. C: Cells were starved and stimulated with 100 nM insulin for 15 min. Glucose uptake was assayed, and results are the means ± SE of three independent experiments. D, E: mRNA samples were prepared, and the FAS (D) and SCD1 (E) levels were analyzed by RT-PCR. The data represent the means ± SE of three independent experiments. F: Cells were starved and stimulated with 100 nM insulin for 15 min. Incorporation of glucose into lipids was assayed, and results are the means ± SE of three independent experiments. **^{a} $P < 0.01$ (compared with CTL); **^{b} $P < 0.01$ (compared with FA2H); *^{a} $P < 0.05$ (compared with CTL); *^{b} $P < 0.05$ (compared with FA2H). NS, nonsignificant (compared with FA2H).
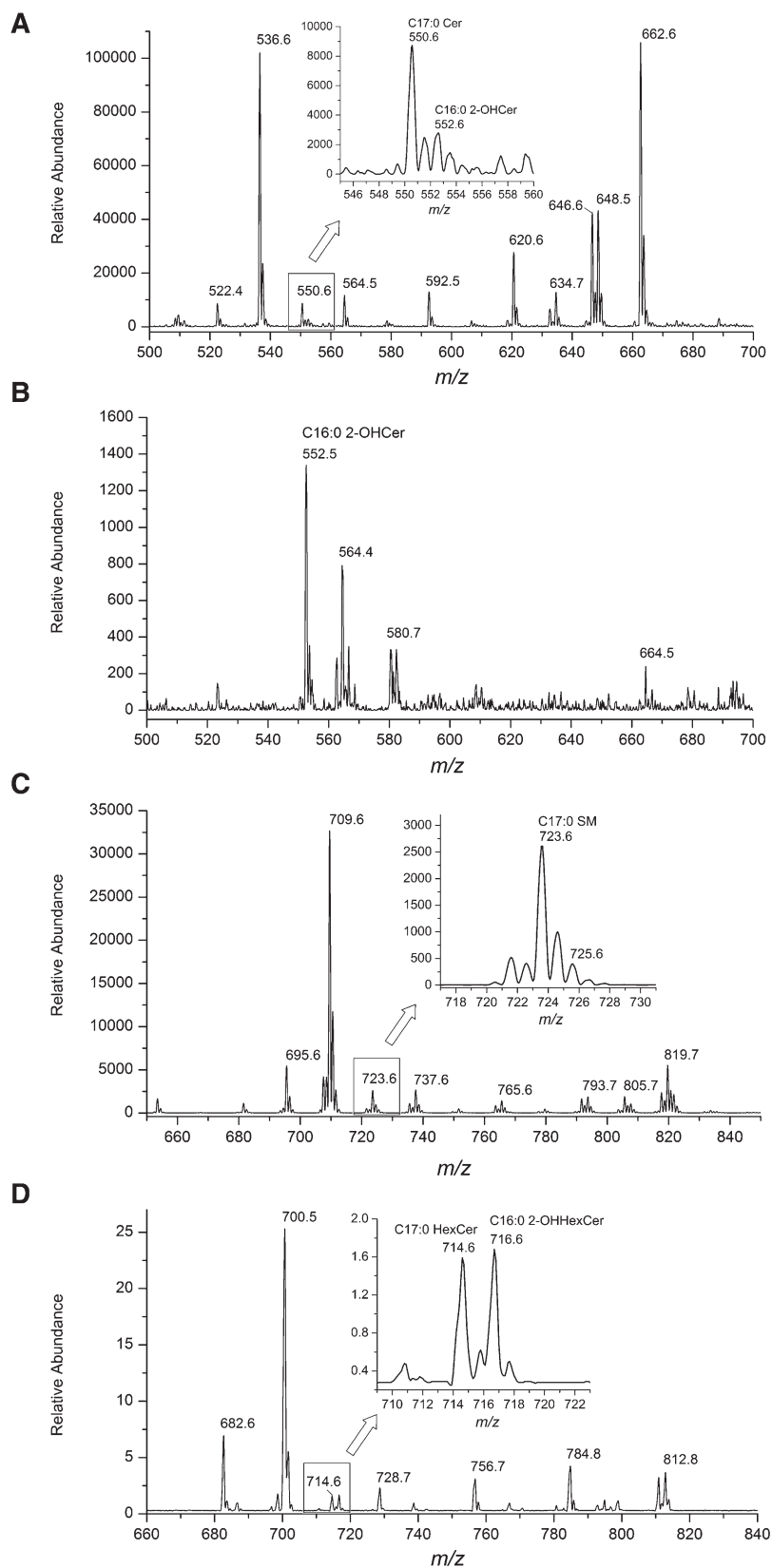
Fig. 5. Identification of sphingolipid species containing 2-OH PA in 3T3-L1 adipocytes. A, B: Total Cer (A) and 2-OH Cer (B) molecular species were fingerprinted by NL scanning of *m/z* 256 (A) or 327 (B) in the negative-ion mode by ESI-MS/MS. C: SM molecular species were fingerprinted by NL scanning of *m/z* 213 in the positive-ion mode by ESI-MS/MS. D: HexCer molecular species were fingerprinted by precursor ion scanning of *m/z* 264 in the positive-ion mode by LC ESI-MS/MS.

major 2-OH Cer species, and the peak at m/z 662 represents predominantly C25:0 Cer. To further confirm the identity of C16:0 2-OH Cer at m/z 552 in the negative-ion mode, we performed the LC MS/MS analysis of C16:0 2-OH Cer in adipocyte extracts, and authentic standard C12:0 2-OH Cer spiked in the lipid extracts as $[M+H]^+$ in the positive-ion mode (21). As we predicted, the multiple reaction monitoring (MRM) chromatograms showed that C16:0 2-OH Cer and the C12:0 2-OH Cer were coeluted (see supplementary Fig. IV). We next identified SM molecular species by the NL scanning of m/z 213 in the positive-ion mode as $[M+Li]^+$ as described (23). The calculated peak of C16:0 2-OH SM is at m/z 725, and its intensity is approximately the same as that of the M+2 isotopic peak of m/z 723 (C17:0 SM) (Fig. 5C), suggesting that the amount of 2-OH PA in SM is minimal. Because we were not able to accurately profile HexCer species by direct infusion, probably due to the presence of the large amount of triacylglycerol (TAG), we used LC MS/MS in the precursor ion scanning mode with specific product ion of a fragment at m/z 264 as described (21). HexCer species were analyzed in the positive-ion mode as $[M+H]^+$. Similar to Cer, significant amounts of HexCer are present in adipocytes, with the most-abundant peak at m/z 700 (C16:0 HexCer) (Fig. 5D). A peak at m/z 716 (C16:0 2-OH HexCer) was identified with peak intensity similar to that at m/z 714 (C17:0 HexCer) (Fig. 5D), suggesting the presence of 2-OH PA in HexCer.

With the knowledge of which sphingolipid species contain 2-OH FAs, we utilized LC MS/MS to specifically quantify C16:0 2-OH Cer and C16:0 2-OH HexCer (21) and studied their regulation by FA2H knockdown and by 2-OH PA enantiomers. FA2H knockdown decreased the amounts of both C16:0 2-OH Cer and C16:0 2-OH HexCer (**Fig. 6**). When 2-OH PA enantiomers were added to FA2H knockdown cells, (R)-2-OH PA was enriched in HexCer (Fig. 6B), whereas (S)-2-OH PA was preferentially incorporated into Cer (Fig. 6A). In contrast, the amounts of nonhydroxy PA in Cer and HexCer were not increased by 2-OH PA (see supplementary Fig. V), suggesting that the differential incorporation of 2-OH PA enantiomers into distinct sphingolipid classes is mainly due to enzyme substrate

specificities instead of altered total enzymatic activities involved in the biosynthesis of Cers and HexCers. Collectively, regulation of raft mobility and GLUT4 level by FA2H and 2-OH PA enantiomers is correlated with the amounts of 2-OH PA in sphingolipids and distribution of 2-OH PA enantiomers in different sphingolipid subclasses.

DISCUSSION

In mammalian cells, two types of FA 2-hydroxylases have been identified: phytanoyl-CoA hydroxylase (27) and FA2H (2, 3). Mammalian FA2H is a NAD(P)H-dependent monooxygenase which was cloned independently by two research groups (2, 3). Its products, 2-OH FAs, are enriched in mammalian sphingolipids, and most studies have been focused on roles of FA2H in generating 2-OH FA-containing sphingolipids (5). The 2-OH FAs produced by FA2H are chiral, and our current study demonstrated that FA2H is stereospecific for the production of (R) enantiomers. Further biophysical study showed that (R)-2-OH PA, but not (S)-2-OH PA reverses enhanced membrane mobility by FA2H knockdown in adipocytes. It is still not clear how sphingolipids containing different 2-OH FA enantiomers have distinct effects on membrane mobility. Based on Pascher's studies (28) on the conformations of 2-OH FA-containing Cers, the different spatial orientation of the hydroxyl group in (R)-2-OH FAs and (S)-2-OH FAs was suggested as the major factor leading to their functional disparity. One possible model is that the (R)-2-hydroxyl group is preferred to participate in intermolecular hydrogen bonding, favoring lipid-lipid interaction, whereas the 2-hydroxyl group of the (S) form is usually involved in an intramolecular hydrogen bonding with adjacent carbonyl oxygen (see supplementary Fig. VI). Accordingly, raft domains enriched in (R)-2-OH sphingolipids are more tightly packed and become less mobile, as compared with those containing more (S)-2-OH sphingolipids, where the steric hindrance caused by the branched loop of intramolecular hydrogen bond attenuates the lipid-lipid packing and thus promotes membrane fluidity. The influence of the chirality
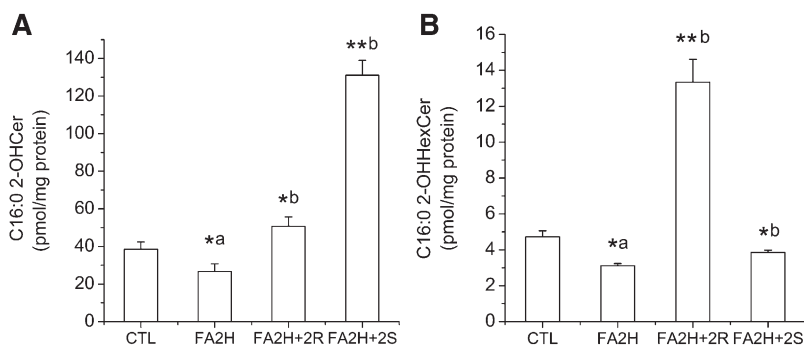

Fig. 6. Regulation of Cer and HexCer containing 2-OH PA by FA2H and 2-OH PA enantiomers. 3T3-L1 adipocytes were treated with a negative control siRNA (CTL) or an siRNA recognizing FA2H (FA2H). Twenty-four hours post transfection, 50 μM (R)-2-OH PA (2R) or (S)-2-OH PA (2S) was added as indicated. C16:0 2-OH Cer and C16:0 2-OH HexCer were quantified by LC ESI-MS/MS, and results are the means ± SE of three independent experiments. *[a] $P < 0.05$ (compared with CTL); *[b] $P < 0.05$ (compared with FA2H); **[b] $P < 0.01$ (compared with FA2H).

of the 2-hydroxyl group of FAs on the lipid-lipid interactions was also supported by the fact that (*R*)-2-OH FA-containing ceramides were self-condensed on the water surface, whereas considerable pressure was required for the condensation of the corresponding (*S*) enantiomer (29). In addition to presenting as a different conformation of a hydroxyl group in sphingolipids, 2-OH FA enantiomers are incorporated into different sphingolipid subclasses. The incorporation of (*R*)-2-OH FAs into HexCer may further favor intermolecular lipid-lipid interaction to form a close-packed condensed phase. This hypothesis will need to be verified by in vitro biophysical experiments. Future studies will also aim to examine how lipid-lipid interaction regulated by FA2H and 2-OH FAs could alter endocytosis and intracellular trafficking pathways.

The data presented in this manuscript demonstrates that regulation of membrane mobility by FA2H and 2-OH PA is in part via the synthesis of 2-OH sphingolipids. However, we cannot exclude other mechanisms that may lead to this regulation. We did not observe changes of average chain length of fatty acyl moieties by FA2H knockdown or 2-OH PA (data not shown), but other changes of membrane composition (e.g., cholesterol, PC/PE ratio, lyso phospholipids, etc.) may contribute to this regulation. FAS and SCD1 levels were regulated by FA2H activity, suggesting involvement of transcriptional regulation. Although caveolin-1 levels are not changed, FA2H may mediate levels of some other proteins in rafts that regulate mobility. A comprehensive proteomic analysis will probably provide valuable information.

Both enantiomers of 2-OH FAs were identified in biological samples, but the specific enzymatic pathways leading to their generation are still not clear. Additional FA2Hs in mammalian cells were indicated in recent studies (10, 30), and identification and characterization of those enzyme(s) will be critical to understanding the metabolism pathways and functions of 2-OH FAs. Our data demonstrated that (*R*)-2-OH PA was enriched in HexCer, whereas (*S*)-2-OH PA was preferentially incorporated into Cer. However, the possibility of their presence in other lipid classes cannot be excluded, and some functions of FA2H could be sphingolipid-independent. This possibility will be examined in future studies with synthesis of proper authentic standards containing 2-OH FA enantiomers. In addition to incorporation into lipid species, 2-OH FAs could be further catabolized by the α oxidation pathway (Scheme 1). In that pathway, 2-OH phytanoyl CoA lyase cleaves 2-OH acyl-CoA to an aldehyde with one less carbon and thiamin pyrophosphate is required for its enzymatic activity (31). It will be interesting to examine the metabolic consequence of the accumulative reactive lipid aldehydes. For example, lipid aldehydes could modify the side chains of protein amino acids in a reaction termed protein carbonylation (32) leading to alteration of glucose tolerance (33).

FA2H is highly expressed in brain and epidermis. Complete absence of 2-OH sphingolipids is associated with late-onset axon and myelin sheath degeneration (9) and causes central nervous system dysfunction (8). In the epidermis, FA2H is required for epidermal lamellar membrane formation during keratinocyte differentiation (34) and fur formation and sebum production in mice (14). Physiological functions of FA2H in other cell types/organs are largely unknown. In agreement with the neuronal dysfunction in FA2H-null mice, mutations in the FA2H gene in humans have recently been identified as associated with leukodystrophy (10), hereditary spastic paraplegia (11), and neurodegeneration (12). However, although the main known effect of total loss of function of FA2H is neuronal, our recent study indicated that the enzyme may play a role in adipocyte metabolism by regulating GLUT4 trafficking, lipogenesis, and adipocyte differentiation (13). The expression of FA2H has also been identified in adipose tissues, and its levels are correlated with adiposity (35). The functions of FA2H and FA 2-hydroxylation in regulating FA α oxidation and adipocyte metabolism and their physiological relevance require future studies. These studies will be facilitated by recent availability of transgenic mouse models.

In summary, we identified for the first time the stereospecificity of FA2H for the exclusive production of (*R*)-enantiomeric 2-OH FAs in mammalian cells. (*R*)-2-OH PA, but not the (*S*) enantiomer, reverses the accelerated raft fluidity, reduced GLUT4 protein level, glucose uptake, and lipogenesis that occur in FA2H knockdown adipocytes. Lipidomic analysis suggests that this regulation is in part via synthesis of 2-OH sphingolipids. The results will probably help in the understanding of the mechanisms underlying recently identified human diseases associated with FA2H mutations, and the use of chiral-specific products of FA2H may lead to novel pharmaceutical and dietary treatments. In addition, this study will direct future studies on the potentially important but unstudied contribution of FA 2-hydroxylation and α oxidation to the regulation of adipocyte metabolism.▮▮

REFERENCES

1. Ekholm, O., S. Jaikishan, M. Lonnfors, T. K. Nyholm, and J. P. Slotte. 2011. Membrane bilayer properties of sphingomyelins with amide-linked 2- or 3-hydroxylated fatty acids. *Biochim. Biophys. Acta.* **1808:** 727–732.
2. Alderson, N. L., B. M. Rembiesa, M. D. Walla, A. Bielawska, J. Bielawski, and H. Hama. 2004. The human FA2H gene encodes a fatty acid 2-hydroxylase. *J. Biol. Chem.* **279:** 48562–48568.
3. Eckhardt, M., A. Yaghootfam, S. N. Fewou, I. Zoller, and V. Gieselmann. 2005. A mammalian fatty acid hydroxylase responsible for the formation of alpha-hydroxylated galactosylceramide in myelin. *Biochem. J.* **388:** 245–254.
4. Foulon, V., M. Sniekers, E. Huysmans, S. Asselberghs, V. Mahieu, G. P. Mannaerts, P. P. Van Veldhoven, and M. Casteels. 2005. Breakdown of 2-hydroxylated straight chain fatty acids via peroxisomal 2-hydroxyphytanoyl-CoA lyase: a revised pathway for the alpha-oxidation of straight chain fatty acids. *J. Biol. Chem.* **280:** 9802–9812.

5. Hama, H. 2010. Fatty acid 2-hydroxylation in mammalian sphingo-lipid biology. *Biochim. Biophys. Acta.* **1801:** 405–414.

6. Hama, H., D. A. Young, J. A. Radding, D. Ma, J. Tang, S. D. Stock, and J. Y. Takemoto. 2000. Requirement of sphingolipid alpha-hydroxylation for fungicidal action of syringomycin E. *FEBS Lett.* **478:** 26–28.

7. Herrero, A. B., A. M. Astudillo, M. A. Balboa, C. Cuevas, J. Balsinde, and S. Moreno. 2008. Levels of SCS7/FA2H-mediated fatty acid 2-hydroxylation determine the sensitivity of cells to antitumor PM02734. *Cancer Res.* **68:** 9779–9787.

8. Potter, K. A., M. J. Kern, G. Fullbright, J. Bielawski, S. S. Scherer, S. W. Yum, J. J. Li, H. Cheng, X. Han, J. K. Venkata, et al. 2011. Central nervous system dysfunction in a mouse model of Fa2h defi-ciency. *Glia.* **59:** 1009–1021.

9. Zoller, I., M. Meixner, D. Hartmann, H. Bussow, R. Meyer, V. Gieselmann, and M. Eckhardt. 2008. Absence of 2-hydroxylated sphingolipids is compatible with normal neural development but causes late-onset axon and myelin sheath degeneration. *J. Neurosci.* **28:** 9741–9754.

10. Edvardson, S., H. Hama, A. Shaag, J. M. Gomori, I. Berger, D. Soffer, S. H. Korman, I. Taustein, A. Saada, and O. Elpeleg. 2008. Mutations in the fatty acid 2-hydroxylase gene are associated with leukodystrophy with spastic paraparesis and dystonia. *Am. J. Hum. Genet.* **83:** 643–648.

11. Dick, K. J., M. Eckhardt, C. Paisan-Ruiz, A. A. Alshehhi, C. Proukakis, N. A. Sibtain, H. Maier, R. Sharifi, M. A. Patton, W. Bashir, et al. 2010. Mutation of FA2H underlies a complicated form of heredi-tary spastic paraplegia (SPG35). *Hum. Mutat.* **31:** E1251–E1260.

12. Kruer, M. C., C. Paisan-Ruiz, N. Boddaert, M. Y. Yoon, H. Hama, A. Gregory, A. Malandrini, R. L. Woltjer, A. Munnich, S. Gobin, et al. 2010. Defective FA2H leads to a novel form of neurodegen-eration with brain iron accumulation (NBIA). *Ann. Neurol.* **68:** 611–618.

13. Guo, L., D. Zhou, K. M. Pryse, A. L. Okunade, and X. Su. 2010. Fatty acid 2-hydroxylase mediates diffusional mobility of raft-asso-ciated lipids, GLUT4 level and lipogenesis in 3T3-L1 adipocytes. *J. Biol. Chem.* **285:** 25438–25447.

14. Maier, H., M. Meixner, D. Hartmann, R. Sandhoff, L. Wang-Eckhardt, I. Zoller, V. Gieselmann, and M. Eckhardt. 2011. Normal fur development and sebum production depends on fatty acid 2-hydroxylase expression in sebaceous glands. *J. Biol. Chem.* **286:** 25922–25934.

15. Jenske, R., and W. Vetter. 2007. Highly selective and sensitive gas chromatography-electron-capture negative-ion mass spectrometry method for the indirect enantioselective identification of 2- and 3-hydroxy fatty acids in food and biological samples. *J. Chromatogr. A.* **1146:** 225–231.

16. Jenske, R., and W. Vetter. 2008. Enantioselective analysis of 2- and 3-hydroxy fatty acids in food samples. *J. Agric. Food Chem.* **56:** 11578–11583.

17. Jenske, R., and W. Vetter. 2009. Concentrations of medium-chain 2- and 3-hydroxy fatty acids in foodstuffs. *Food Chem.* **114:** 1122–1129.

18. Su, X., I. J. Lodhi, A. R. Saltiel, and P. D. Stahl. 2006. Insulin-stimulated interaction between insulin receptor substrate 1 and p85alpha and activation of protein kinase B/Akt require Rab5. *J. Biol. Chem.* **281:** 27982–27990.

19. Szponar, B., E. Norin, T. Midtvedt, and L. Larsson. 2002. Limitations in the use of 3-hydroxy fatty acid analysis to determine endotoxin in mammalian samples. *J. Microbiol. Methods.* **50:** 283–289.

20. Yusufoglu, A. 1995. Resolution and resolution efficiencies of 2-, 3-hydroxyhexadecanoic acids. *Chimica Acta Turcica.* **23:** 189–193.

21. Shaner, R. L., J. C. Allegood, H. Park, E. Wang, S. Kelly, C. A. Haynes, M. C. Sullards, and A. H. Merrill, Jr. 2009. Quantitative analysis of sphingolipids for lipidomics using triple quadrupole and quadrupole linear ion trap mass spectrometers. *J. Lipid Res.* **50:** 1692–1707.

22. Han, X. 2002. Characterization and direct quantitation of ceramide molecular species from lipid extracts of biological samples by elec-trospray ionization tandem mass spectrometry. *Anal. Biochem.* **302:** 199–212.

23. Hsu, F. F., and J. Turk. 2000. Structural determination of sphingo-myelin by tandem mass spectrometry with electrospray ionization. *J. Am. Soc. Mass Spectrom.* **11:** 437–449.

24. Gonzalez-Munoz, E., C. Lopez-Iglesias, M. Calvo, M. Palacin, A. Zorzano, and M. Camps. 2009. Caveolin-1 loss of function accel-erates glucose transporter 4 and insulin receptor degradation in 3T3-L1 adipocytes. *Endocrinology.* **150:** 3493–3502.

25. Liu, L., D. Brown, M. McKee, N. K. Lebrasseur, D. Yang, K. H. Albrecht, K. Ravid, and P. F. Pilch. 2008. Deletion of Cavin/PTRF causes global loss of caveolae, dyslipidemia, and glucose intoler-ance. *Cell Metab.* **8:** 310–317.

26. Foufelle, F., B. Gouhot, J. P. Pegorier, D. Perdereau, J. Girard, and P. Ferre. 1992. Glucose stimulation of lipogenic enzyme gene ex-pression in cultured white adipose tissue. A role for glucose 6-phos-phate. *J. Biol. Chem.* **267:** 20543–20546.

27. Wanders, R. J., G. A. Jansen, and M. D. Lloyd. 2003. Phytanic acid alpha-oxidation, new insights into an old problem: a review. *Biochim. Biophys. Acta.* **1631:** 119–135.

28. Pascher, I. 1976. Molecular arrangements in sphingolipids. Conformation and hydrogen bonding of ceramide and their im-plication on membrane stability and permeability. *Biochim. Biophys. Acta.* **455:** 433–451.

29. Lofgren, H., and I. Pascher. 1977. Molecular arrangements of sphingolipids. The monolayer behaviour of ceramides. *Chem. Phys. Lipids.* **20:** 273–284.

30. Dan, P., S. Edvardson, J. Bielawski, H. Hama, and A. Saada. 2011. 2-Hydroxylated sphingomyelin profiles in cells from patients with mutated fatty acid 2-hydroxylase. *Lipids Health Dis.* **10:** 84.

31. Casteels, M., M. Sniekers, P. Fraccascia, G. P. Mannaerts, and P. P. Van Veldhoven. 2007. The role of 2-hydroxyacyl-CoA lyase, a thia-min pyrophosphate-dependent enzyme, in the peroxisomal metab-olism of 3-methyl-branched fatty acids and 2-hydroxy straight-chain fatty acids. *Biochem. Soc. Trans.* **35:** 876–880.

32. Nystrom, T. 2005. Role of oxidative carbonylation in protein qual-ity control and senescence. *EMBO J.* **24:** 1311–1317.

33. Grimsrud, P. A., M. J. Picklo, Sr., T. J. Griffin, and D. A. Bernlohr. 2007. Carbonylation of adipose proteins in obesity and insulin resis-tance: identification of adipocyte fatty acid-binding protein as a cel-lular target of 4-hydroxynonenal. *Mol. Cell. Proteomics.* **6:** 624–637.

34. Uchida, Y., H. Hama, N. L. Alderson, S. Douangpanya, Y. Wang, D. A. Crumrine, P. M. Elias, and W. M. Holleran. 2007. Fatty acid 2-hydroxylase, encoded by FA2H, accounts for differentiation-asso-ciated increase in 2-OH ceramides during keratinocyte differentia-tion. *J. Biol. Chem.* **282:** 13211–13219.

35. Koza, R. A., L. Nikonova, J. Hogan, J. S. Rim, T. Mendoza, C. Faulk, J. Skaf, and L. P. Kozak. 2006. Changes in gene expression fore-shadow diet-induced obesity in genetically identical mice. *PLoS Genet.* **2:** e81.